


# Experimental Observation of Modal-Dispersion-Induced FWM Efficiency Increase and Non-linearity Coefficient Characterization in Deployed

Downloaded from: https://research.chalmers.se, 2026-11-27 10:03 UTC

Citation for the original published paper (version of record):

Alves Zischler, L., Lasagni, C., Raj, M. et al (2026). Experimental Observation of Modal-Dispersion-Induced FWM Efficiency Increase and Non-linearity Coefficient Characterization in Deployed Coupled-Core Multi-Core Fibers. 2026 European Conference on Optical Communications (ECOC)

N.B. When citing this work, cite the original published paper.

research.chalmers.se offers the possibility of retrieving research publications produced at Chalmers University of Technology. It covers all kind of research output: articles, dissertations, conference papers, reports etc. since 2004. research.chalmers.se is administrated and maintained by Chalmers Library

(article starts on next page)

# Experimental Observation of Modal-Dispersion-Induced FWM Efficiency Increase and Non-linearity Coefficient Characterization in Deployed Coupled-Core Multi-Core Fibers

Lucas Alves Zischler[(1,*)], Chiara Lasagni[(2)], Manish Raj[(3)], Giammarco Di Sciullo[(1)], Magnus Karlsson[(3)], Paolo Serena[(2)], Alberto Bononi[(2)], Tetsuya Hayashi[(4)], Antonio Mecozzi[(1)], and Cristian Antonelli[(1)]

[(1)] University of L'Aquila, L'Aquila, Italy, [*]lucas.zischler@univaq.it
[(2)] Università degli Studi di Parma, Parma, Italy,
[(3)] Chalmers University of Technology, Göteborg, Sweden,
[(4)] Sumitomo Electric Industries, Ltd., Yokohama, Japan.

***Abstract*** *We experimentally observe enhanced four-wave mixing efficiency induced by spatial-mode dispersion at large channel spacing in a field-deployed coupled-core 4-core fiber, consistent with the theory. We characterize the MCF effective non-linearity coefficient, demonstrating a 4.26-fold reduction against a co-deployed single-mode fiber. ©2026 The Author(s)*

## Introduction

Rising data rate requirements have motivated the development of novel fiber designs that provide additional orthogonal propagation paths within the standard $125\,\mu\mathrm{m}$ cladding diameter[1]. Within space-division multiplexing (SDM) fiber designs, multi-core fibers (MCF) offer flexibility in the degree of coupling between spatial modes. Uncoupled-core MCFs do not require multiple-input multiple-output (MIMO) equalization, but require significant spacing between cores or low-refractive-index trenches, reducing the achievable core count within a given cladding radius. In contrast, coupled-core MCFs offer higher information rate density but rely on MIMO filtering[2].

In coupled-core MCFs, the optical fields excited in each core rapidly spread across all cores. When uncorrelated signals are transmitted, the effective intensity of non-linear distortions is generally reduced compared with an equivalent single-mode fiber (SMF)[3,4]. Small refractive index variations between cores induce spatial-mode dispersion (SMD), which is typically much larger than the polarization-mode dispersion observed in SMF. Although the dominant non-linear contributions from self- and cross-phase modulation generally weakens with SMD, theoretical analyses[5] have shown that SMD increases specifically the 3- and 4-channel four-wave-mixing (FWM) efficiency in MCFs relative to the dispersionless case, an effect accurately captured by the ergodic Gaussian-noise (GN) model[5,6]. While the core-count-induced efficiency reduction remains configuration-independent, the SMD-induced increase becomes dominant at large channel spacings.

In this work, we experimentally observe the SMD-induced increase in FWM efficiency as well as the four-fold reduction of the non-linearity coefficient in a coupled-core 4-core fiber field-deployed in L'Aquila, Italy[7]. The results are also validated by comparison with SMF measurements and split-step Fourier method (SSFM) simulations. Additionally, measurements where SMD impairments are negligible are further validated using closed-form analytical solutions, obtained by expanding on recent SMF studies[8]. The analytical solution is further employed to characterize the effective non-linearity coefficient of the MCF. Prior characterizations of this coefficient were limited to short spools of $1\,\mathrm{km}$ or less and required narrowly spaced lasers to reduce modal-dispersion-induced decorrelation, measuring efficiency via the non-linear phase shift[9]. In contrast, in this work we extract the non-linearity coefficient, for the first time, from a $69.3$-$\mathrm{km}$-long field-deployed MCF link.

## Theory

In a strongly coupled MCF, considering continuous-wave (CW) signals at discrete frequencies, the generalized Jones vector field $\vec{E}_i$ at $f_i$ evolves according to the multi-component Manakov equation[6,10,11]

$$\frac{\mathrm{d}\vec{E}_i}{\mathrm{d}z} = \left(\frac{-\alpha_i}{2} - j\beta_i + \mathbf{H}_i\right)\vec{E}_i + j\kappa\bar{\gamma}\sum_{f_h - f_k + f_l = f_i} \vec{E}_h \vec{E}_k^{\dagger} \vec{E}_l, \quad (1)$$

where $\alpha_i$ and $\beta_i$ represent the core-averaged power attenuation coefficient and propagation constant, respectively. The matrix $\mathbf{H}_i$ is a $z$- and frequency-dependent random unitary matrix accounting for crosstalk and stochastic variations in core propagation constants, resulting in SMD[12,13]. The dagger $(\cdot)^{\dagger}$ denotes Hermitian conjugate, and $\kappa\bar{\gamma}$, where $\kappa \approx \frac{4}{3}\left(\frac{2N}{2N+1}\right)$ with $N$ the core count,

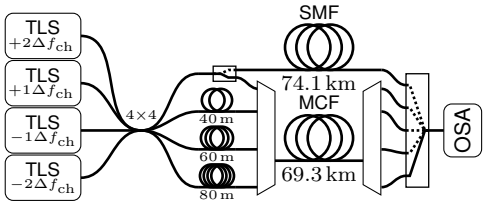


**Fig. 1:** Diagram of the experimental setup.

represents the non-linearity coefficient accounting for the fast-averaging dynamics among the $2N$ space and polarization modes[4,14]. The characterization of $\bar{\gamma}$ is one of the goals of this work. This coefficient accounts for the average interaction across the cores' field profiles, and, for $N$ homogeneous cores, it is given by[4]

$$\bar{\gamma} = \frac{2\pi f_0 \mathrm{n}_2}{cNA_{\mathrm{eff}}}, \tag{2}$$

where $f_0$ is the central optical frequency, $n_2$ is the material non-linear refractive index, $c$ is the speed of light, and $A_{\mathrm{eff}}$ is the cores' effective area.

Within the region where the SMD effect is negligible, and assuming that the fields at $f_h$, $f_k$, and $f_l$ are non-depleting and evolving linearly (governed solely by attenuation and propagation phase), the core-averaged FWM optical power at $f_i$ can be expressed in closed form as[15,16]

$$P_i^{\mathrm{FWM}} = \frac{\kappa^2\bar{\gamma}^2}{N^2} \sum_{f_h - f_k + f_l = f_i} \zeta_h P_h P_k P_l \chi_{ihkl}, \tag{3}$$

where $P_h$ denotes the total launch power (summed over all spatial modes) for the frequency channel $f_h$, $\zeta_h$ equals the signal kurtosis[17] at $f_h$ if $f_h = f_l$ and otherwise $\zeta_h = 4N$, and $\chi_{ihkl}$ represents the longitudinal component of the FWM term

$$\chi_{ihkl} = \frac{e^{\Delta\alpha L} - 2e^{\frac{1}{2}\Delta\alpha L}\cos(\Delta\beta L) + 1}{\Delta\alpha^2 + 4\Delta\beta^2} e^{-\alpha_i L}, \tag{4}$$

with $L$ being the fiber length. The coefficients $\Delta\alpha$ and $\Delta\beta$ are

$$\begin{aligned} \Delta\alpha &= \alpha_i - \alpha_h - \alpha_k - \alpha_l, \\ \Delta\beta &\approx 2\pi^2 \beta_{2,i} \left(i^2 - h^2 + k^2 - l^2\right) \Delta f_{\mathrm{ch}}^2, \end{aligned} \tag{5}$$

where the second-order Taylor expansion for the propagation constant mismatch $\Delta\beta$ was used, with $\Delta f_{\mathrm{ch}}$ denoting the channel spacing, and $i, h, k, l \in [1, N_{\mathrm{ch}}]$ the channel indices within $N_{\mathrm{ch}}$ evenly spaced slots.

For experimental evaluation, from (3), we introduce the normalized FWM power, scaled by the core-averaged received optical power, as

$$P_{\mathrm{Norm}}^{\mathrm{FWM}} = \frac{\kappa^2\bar{\gamma}^2}{4N} \sum_{f_h - f_k + f_l = f_i} \frac{\zeta_h P_{\mathrm{TX}}^2 (e^{-2\alpha L} + 1) e^{-\alpha L}}{\alpha^2 + \Delta\beta^2}, \tag{6}$$

where we assume equal launch power $P_{\mathrm{TX}}$ for all channels, flat attenuation profile ($\alpha_i = \alpha$), and use the linear average approximation for $\chi_{ihkl}$, which is accurate at practical transmission distances[8,16].

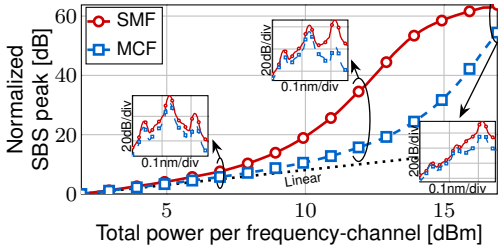


**Fig. 2:** Measured SBS peak power versus total channel power for both fibers. The dotted line indicates the linear trend, and insets show OSA traces for the specified power values.

## Experimental setup

Figure 1 shows the experimental setup. Each output of a $4\times4$ coupler carries identical copies of four tones from as many tunable laser sources (TLS). Delay lines decorrelate the signals for each core. Power values are set at the laser output, with $1.92\,\mathrm{dB}$ insertion loss to the fiber input. The MCF setup has an additional $1.16\,\mathrm{dB}$ loss due to additional patch cords and the fan-in/fan-out devices. For SMF measurements, a single coupler output is used, maintaining approximately equal power per core across both fibers. The FWM is measured at $193\,\mathrm{THz}$, with four CW tones allocated at $\pm2\Delta f_{\mathrm{ch}}$ and $\pm1\Delta f_{\mathrm{ch}}$ relative to the channel under test. Received and transmitted spectra are measured using an optical spectrum analyzer (OSA) and normalized to the average CW received peak power. Therefore, the receiver power values are compensated for losses and normalized to the launch power.

As we use unmodulated $100\text{-kHz}$-width tones, we characterize the stimulated Brillouin scattering (SBS) threshold to define the safe operating region, avoiding power suppression and backreflection. Figure 2 shows a plot of the backscattered SBS power, normalized to the lowest measurement, versus per-channel power. In the MCF, the laser field is launched into a single core, as the optical power rapidly spreads across all the cores as a result of the strong mode mixing. The figure shows an increase in the SBS threshold for the MCF, when considering total launch power values.

## SMD-induced FWM efficiency increase

Figure 3 shows measured normalized spectra for $15\,\mathrm{dBm}$ per core ($9\,\mathrm{dBm}$ per CW tone per core) alongside SSFM simulations for the MCF.

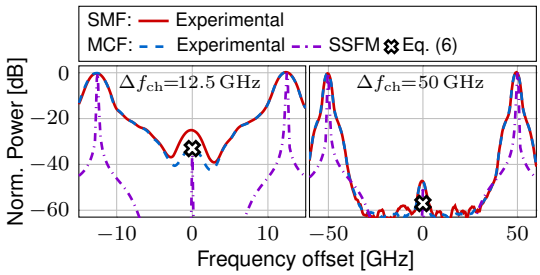


**Fig. 3:** Normalized power spectra from experiments and theory for two distinct spacings, centered at the channel under test.

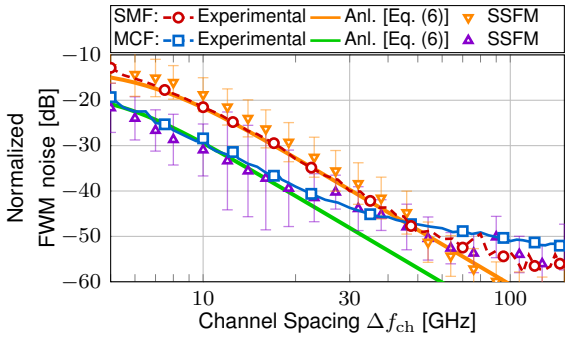


**Fig. 4:** Normalized FWM noise power versus channel spacing for both fibers. Error bars on SSFM curves represent one sample standard deviation across Monte Carlo trials.

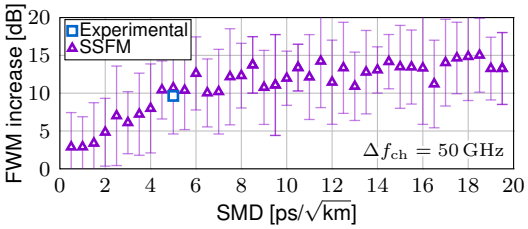


**Fig. 5:** Four-wave-mixing noise increase versus modal dispersion relative to the analytical curve (Eq. (6)) for the MCF. Error bars on SSFM curves represent one sample standard deviation across Monte Carlo trials.

The SSFM simulations uses 1000 frequency bins, where the 4 CW tones are modeled as Gaussian-distributed signals. Random coupling and SMD are accounted for with a waveplate model. We consider $5\,\mathrm{ps}/\sqrt{\mathrm{km}}$ of SMD as previously characterized for the fiber under test[18]. Results are averaged over 10 Monte Carlo trials. The cross marks show the analytical solution from Eq. (6) at the center frequency. Attenuation is measured as $0.227\,\mathrm{dB/km}$ for the MCF, and $0.246\,\mathrm{dB/km}$ for the SMF. The parameter $\beta_2$ is set to $-24.4\,\mathrm{ps^2/km}$ for the MCF, as per manufacturer's estimate, and to $-21.7\,\mathrm{ps^2/km}$ for the SMF. The values for $\bar{\gamma}$ used in the theoretical curves are discussed throughout the rest of this work.

The FWM peak seen in Fig. 3 for the MCF is reduced compared to the SMF at $12.5\,\mathrm{GHz}$ channel spacing but approaches similar values at $50\,\mathrm{GHz}$. Split-step results agree well with the experimental data for both fiber types and spacings. However, the cross marker underestimates the FWM noise power at $50\,\mathrm{GHz}$ since Eq. (6) neglects SMD.

Figure 4 shows measured normalized FWM noise versus channel spacing, alongside SSFM simulations and the analytical solution from Eq. (6). For the MCF, all three curves agree well up to $20\,\mathrm{GHz}$. Above this threshold, SMD significantly enhances FWM efficiency and Eq. (6) becomes inaccurate, but excellent agreement between data and SSFM simulations remains.

Figure 5 plots the FWM enhancement versus SMD for the MCF at $15\,\mathrm{dBm}$ power per core, normalized to the dispersionless case from Eq. (6). The enhancement increases with SMD up to a saturation value, consistent with prior predictions utilizing the ergodic GN model[5,6].

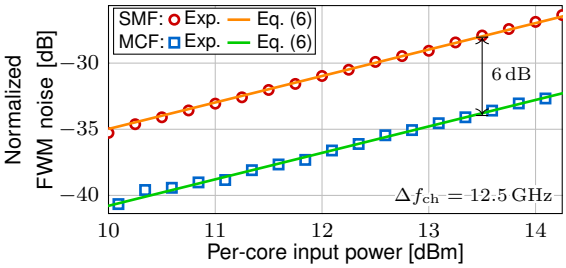


**Fig. 6:** Normalized FWM noise versus input power per core at $12.5\,\mathrm{GHz}$ channel spacing.

### Estimation of the non-linearity coefficient

Considering all other fiber parameters known, $\bar{\gamma}$ can be analytically estimated from Eq. (6) as

$$\bar{\gamma} = \frac{2}{\kappa}\sqrt{\frac{N P_{\mathrm{Norm}}^{\mathrm{FWM}}}{\sum_{f_h - f_k + f_l = f_i} \frac{\zeta_h P_{\mathrm{TX}}^2 (e^{-2\alpha L}+1) e^{-\alpha L}}{\alpha^2 + \Delta\beta^2}}}. \quad (7)$$

With Eq. (7), the effective non-linearity coefficient is estimated by fitting measurements of the normalized FWM power at $12.5\,\mathrm{GHz}$ (where the SMD effect is negligible) from a launch power sweep. The result of this procedure is shown in Fig. 6. From the measured data, we estimate $\bar{\gamma}$ as $1.318/\mathrm{W/km}$ and $0.286/\mathrm{W/km}$, for the SMF and MCF respectively. The SMF value is within standard range, and accounting for the distinct effective mode areas[19,20] (SMF: $75\,\mu\mathrm{m}^2$, MCF: $81\,\mu\mathrm{m}^2$ per core), the MCF exhibits a 4.26-fold reduction in the effective non-linearity coefficient. A fourfold reduction is expected from core multiplicity alone[4] as seen in Eq. (2), with the additional suppression possibly due to differing doping concentrations. These results align with theoretical predictions[4] and prior experimental report[9].

### Conclusions

Spatial-mode dispersion influences non-linear interactions in SDM fibers, resulting in enhanced FWM contributions at large frequency spacings. In this work, we have experimentally demonstrated the SMD-induced FWM increase, validating prior theoretical predictions. Additionally, our measurements have enabled the characterization of the non-linearity coefficient in a field-deployed MCF link, revealing a core-count-proportional reduction consistent with theory.

### Acknowledgements

Funded by the European Union (Grant Agreement 101120422 and 101072409). Views and opinions expressed are, however, those of the author(s) only and do not necessarily reflect those of the European Union or REA. Neither the European Union nor the granting authority can be held responsible for them.

## References


[1] P. J. Winzer, "Optical networking beyond WDM", *IEEE Photonics Journal*, vol. 4, no. 2, pp. 647–651, 2012. DOI: 10.1109/JPHOT.2012.2189379.

[2] K. Saitoh and S. Matsuo, "Multicore fiber technology", *Journal of lightwave technology*, vol. 34, no. 1, pp. 55–66, 2016. DOI: 10.1109/JLT.2015.2466444.

[3] R. Ryf et al., "Long-Haul Transmission over Multi-Core Fibers with Coupled Cores", in *2017 European Conference on Optical Communication (ECOC)*, 2017, pp. 1–3. DOI: 10.1109/ECOC.2017.8345874.

[4] C. Antonelli, M. Shtaif, and A. Mecozzi, "Modeling of nonlinear propagation in space-division multiplexed fiber-optic transmission", *Journal of Lightwave Technology*, vol. 34, no. 1, pp. 36–54, 2015. DOI: 10.1109/JLT.2015.2510511.

[5] C. Lasagni, P. Serena, A. Bononi, A. Mecozzi, and C. Antonelli, "On the impact of four-wave mixing in coupled-core multicore fiber transmissions", in *Optical Fiber Communication Conference*, Optica Publishing Group, 2025, M1H–3. DOI: 10.1364/OFC.2025.M1H.3.

[6] P. Serena, C. Lasagni, A. Bononi, C. Antonelli, and A. Mecozzi, "The ergodic GN model for space-division multiplexing with strong mode coupling", *Journal of Lightwave Technology*, vol. 40, no. 10, pp. 3263–3276, 2022. DOI: 10.1109/JLT.2022.3160207.

[7] C. Antonelli et al., "Field transmission performance of multi-core and few-mode fibers", in *Optical Fiber Communication Conference*, Optica Publishing Group, 2024, W3J–1.

[8] L. A. Zischler et al., "Experimental Characterization and Model Validation of Interference in Classical-QKD Coexistence Transmission", in *2026 Conference on Lasers and Electro-Optics (CLEO)*, 2026, pp. 1–2.

[9] T. Sakamoto, R. Imada, and K. Nakajima, "Characterization of effective nonlinear coefficient in randomly coupled multi-core fiber", *Journal of Lightwave Technology*, vol. 42, no. 13, pp. 4659–4665, 2024. DOI: 10.1109/JLT.2024.3374766.

[10] A. Mecozzi, C. Antonelli, and M. Shtaif, "Nonlinear propagation in multi-mode fibers in the strong coupling regime", *Optics express*, vol. 20, no. 11, pp. 11 673–11 678, 2012. DOI: 10.1364/OE.20.011673.

[11] C. Antonelli, O. Golani, M. Shtaif, and A. Mecozzi, "Nonlinear interference noise in space-division multiplexed transmission through optical fibers", *Optics Express*, vol. 25, no. 12, pp. 13 055–13 078, 2017. DOI: 10.1364/OE.25.013055.

[12] C. Antonelli, A. Mecozzi, M. Shtaif, and P. J. Winzer, "Stokes-space analysis of modal dispersion in fibers with multiple mode transmission", *Optics express*, vol. 20, no. 11, pp. 11 718–11 733, 2012. DOI: 10.1364/OE.20.011718.

[13] C. Antonelli, A. Mecozzi, M. Shtaif, N. K. Fontaine, H. Chen, and R. Ryf, "Stokes-space analysis of modal dispersion of SDM fibers with mode-dependent loss: Theory and experiments", *Journal of Lightwave Technology*, vol. 38, no. 7, pp. 1668–1677, 2019. DOI: 10.1109/JLT.2019.2959191.

[14] A. Mecozzi, C. Antonelli, and M. Shtaif, "Nonlinear equations of propagation in multi-mode fibers with random mode coupling", in *39th European Conference and Exhibition on Optical Communication (ECOC 2013)*, IET, 2013, pp. 1–3. DOI: 10.1049/CP.2013.1453.

[15] L. A. Zischler et al., "Accurate and Effective Model for Coexistence of Classical and Quantum Signals In Optical Fibers", *arXiv preprint arXiv:2510.02807*, 2025.

[16] L. A. Zischler, A. Ghazisaeidi, A. Mecozzi, and C. Antonelli, "Secret Key Rate Limits in Coexisting Classical-Quantum Optical Links", *arXiv preprint arXiv:2602.21671*, 2026.

[17] D. Semrau, E. Sillekens, R. I. Killey, and P. Bayvel, "A modulation format correction formula for the Gaussian noise model in the presence of inter-channel stimulated Raman scattering", *Journal of Lightwave Technology*, vol. 37, no. 19, pp. 5122–5131, 2019. DOI: 10.1109/JLT.2019.2929461.

[18] M. Cappelletti et al., "Statistical analysis of modal dispersion in field-installed coupled-core fiber link", *Journal of Lightwave Technology*, vol. 42, no. 11, pp. 4103–4109, 2024. DOI: 10.1109/JLT.2024.3361088.

[19] T. Hayashi et al., "Field-deployed multi-core fiber testbed", in *2019 24th OptoElectronics and Communications Conference (OECC) and 2019 International Conference on Photonics in Switching and Computing (PSC)*, IEEE, 2019, pp. 1–3. DOI: 10.23919/PS.2019.8818058.

[20] G. Di Sciullo et al., "Characterization of Stimulated Raman Scattering in Field-Deployed Coupled-Core Multi-Core Fibers", *Journal of Lightwave Technology*, vol. 44, no. 2, pp. 550–557, 2026. DOI: 10.1109/JLT.2025.3633510.